

Phytoplankton growth and the interaction of light and temperature: A synthesis at the species and community level

Kyle F. Edwards,^{*1} Mridul K. Thomas,² Christopher A. Klausmeier,³ Elena Litchman⁴

¹Department of Oceanography, University of Hawaii, Honolulu, Hawaii

²Department of Aquatic Ecology, Eawag: Swiss Federal Institute of Aquatic Science and Technology, Zurich, Switzerland

³Department of Plant Biology, Kellogg Biological Station, Michigan State University, Hickory Corners, Michigan

⁴Department of Zoology, Kellogg Biological Station, Michigan State University, Hickory Corners, Michigan

Abstract

Temperature strongly affects phytoplankton growth rates, but its effect on communities and ecosystem processes is debated. Because phytoplankton are often limited by light, temperature should change community structure if it affects the traits that determine competition for light. Furthermore, the aggregate response of phytoplankton communities to temperature will depend on how changes in community structure scale up to bulk rates. Here, we synthesize experiments on 57 phytoplankton species to analyze how the growth-irradiance relationship changes with temperature. We find that light-limited growth, light-saturated growth, and the optimal irradiance for growth are all highly sensitive to temperature. Within a species, these traits are co-adapted to similar temperature optima, but light-limitation reduces a species' temperature optimum by ~5°C, which may be an adaptation to how light and temperature covary with depth or reflect underlying physiological correlations. Importantly, the maximum achievable growth rate increases with temperature under light saturation, but not under strong light limitation. This implies that light limitation diminishes the temperature sensitivity of bulk phytoplankton growth, even though community structure will be temperature-sensitive. Using a database of primary production incubations, we show that this prediction is consistent with estimates of bulk phytoplankton growth across gradients of temperature and irradiance in the ocean. These results indicate that interactions between temperature and resource limitation will be fundamental for explaining how phytoplankton communities and biogeochemical processes vary across temperature gradients and respond to global change.

Global warming has underscored the need to understand how temperature affects organisms, populations, communities, and ecosystems. Predicting the ecological effects of temperature is difficult, in part because populations are typically limited by competition or predation, and so to predict growth or abundance we need to know how temperature modulates the multiple physiological processes that underlie species interactions (Vasseur and McCann 2005; Kordas et al. 2011; O'Connor et al. 2011). For example, simple scaling relationships for the temperature-dependence of ecosystem processes may only apply when resources are not limiting (Xu et al. 2004; López-Urrutia and Morán 2007; De Castro and Gaedke 2008). Although resource limitation and other processes complicate the role of temperature, there still may

be general rules for how temperature modulates physiology and species interactions, and quantifying such rules will enhance our ability to explain ecosystem responses to temperature gradients (Dell et al. 2014). Because light and nutrient limitation strongly affect primary producers, it is essential to characterize any general patterns for how temperature interacts with limitation by these resources.

In this study, we synthesize monoculture experiments that characterize the interactive effects of light and temperature on phytoplankton growth. Phytoplankton contribute nearly half of global primary production, are the base of the food web in aquatic environments, and play a critical role in the feedbacks of the global carbon cycle to anthropogenic forcing (Falkowski et al. 1998; Field et al. 1998). Phytoplankton are very sensitive to environmental change (Doney et al. 2012), and both temperature and irradiance are among the key environmental drivers whose distribution is predicted to continue changing in the future (De Stasio et al. 1996; Boyd et al. 2015). The temperature and irradiance that

*Correspondence: kfe@hawaii.edu

Additional Supporting Information may be found in the online version of this article.

phytoplankton experience tend to be positively correlated, because solar radiation increases water temperature, and increased temperature drives stratification and shoals the mixed layer, thus increasing average irradiance experienced by phytoplankton. Nonetheless, phytoplankton occur over a wide range of temperature-irradiance combinations, including low irradiance at the deep chlorophyll maximum or below in warm waters (Fennel and Boss 2003; Cullen 2015), and saturating irradiance in shallow mixed layers in cold waters (e.g., due to meltwater in the summer in polar regions; Lancelot et al. 1993). Therefore, understanding the processes that control individual growth, community structure, and primary production requires us to understand how light and temperature interact, i.e., how temperature modulates the growth-irradiance relationship and how light modulates the growth-temperature relationship. Whether temperature has important direct effects on phytoplankton growth and community size structure in the ocean is currently debated (Morán et al. 2010; Marañón et al. 2012, 2014; Regaudie-de-Goux and Duarte 2012), and conflicting results may in part be driven by interactions between temperature and resource limitation.

The independent effects of irradiance and temperature on phytoplankton growth have been intensively studied and are well-characterized. Growth increases nearly linearly at low irradiance, saturates at some optimal irradiance for growth, and then declines due to photoinhibition (Langdon 1988; Talmy et al. 2013; Edwards et al. 2015). Interspecific differences in this relationship are thought to be due to differences in pigment content, respiratory costs, cell size, and pathways for photoprotection and repair of photodamage (Langdon 1988; Six et al. 2007). Temperature responses are also unimodal, typically with a left-skew such that growth increases exponentially or linearly from low temperature, and declines more rapidly above the optimum (Eppley 1972; Montagnes et al. 2003; Thomas et al. 2012). Interspecific differences in this relationship are thought to be due to differences in protein structure (particularly the stability of enzymes, which is related to specificity and reaction rates), lipid composition of cell membranes, and chaperone protein production (Clarke 2003; Kingsolver 2009). For both irradiance and temperature responses, differences between genotypes or species measured in the lab have been correlated with differences in distributions across depths, seasons, or latitudes (Rodríguez et al. 2005; Johnson et al. 2006; Thomas et al. 2012, 2016; Edwards et al. 2013a,b).

The interactive effects of temperature and irradiance on phytoplankton have been studied in many experiments (e.g., Dauta 1982; Verity 1982; Palmisano et al. 1987), but there is currently no clear consensus for how growth-irradiance relationships change with temperature, or how thermal optima change with irradiance. It is often expected that light-limited photosynthesis and growth will be less sensitive to temperature than light-saturated rates, due to limitation of

photosynthesis by photon absorption at low irradiance, but contradictory results have been observed (Raven and Geider 1988; Davison 1991; Nicklisch et al. 2008). Phytoplankton growth is often modeled as an exponential function of temperature under all resource conditions (Blackford et al. 2004; Taucher and Oschlies 2011), which assumes that resource-saturated growth has the same monotonic temperature sensitivity as light- or nutrient-limited growth. In contrast, the initial slope of the chlorophyll-specific photosynthesis-irradiance curve is sometimes modeled as temperature-insensitive, while the maximum rate of photosynthesis is given an exponential temperature dependence (Geider et al. 1998; Moore et al. 2002). Importantly, the way in which temperature effects are modeled has large effects on projections of global primary production under climate change (Sarmiento et al. 2004; Taucher and Oschlies 2011).

Many pressing ecological questions require us to “scale up” from community diversity and dynamics to aggregate ecosystem processes. For example, to understand the role of the biosphere in the global carbon cycle we need to know how complex communities respond to multiple environmental factors, and how community structure determines aggregate processes like primary production or carbon export to the deep ocean (Duffy and Stachowicz 2006; Boyd et al. 2015; Worden et al. 2015). Responses to temperature are an area where the difference between individual and aggregate outcomes are significant: even though individual species exhibit unimodal responses to temperature (Thomas et al. 2012; Dell et al. 2014), bulk ecosystem rates typically change monotonically with temperature, i.e., they do not decline above some optimum. This difference between species and community response was explained in an influential paper by Eppley (1972), which compiled measurements of phytoplankton growth rate as a function of temperature. Although individual species exhibited unimodal responses to temperature, the highest observed growth rates across species as a function of temperature increased exponentially. He characterized this with an exponential curve, $\mu = 0.59 \times 10^{0.0275 \times T}$, where μ is specific growth rate (d^{-1}) and T is temperature ($^{\circ}\text{C}$). This curve is equivalent to a Q_{10} of 1.88, i.e., growth increases by a factor of 1.88 when temperature increases by 10°C (a recent update using more data by Bissinger et al. (2008) found an essentially identical exponent, $\mu = 0.81 \times 10^{0.0274 \times T}$, or $Q_{10} = 1.88$). This result implies that species will replace one another along a temperature gradient via competition, with the result that phytoplankton whole-community growth rate increases monotonically with temperature, if the maximum possible growth rate is higher for species adapted to higher temperatures (Eppley 1972; Norberg 2004; Bissinger et al. 2008). We will refer to the predicted whole-community curve, derived from the upper envelope of the single-species curves, as a trait envelope (Fig. 1A). Importantly, it is possible that the shape or slope of this envelope changes as a function of resource limitation (Fig. 1B).

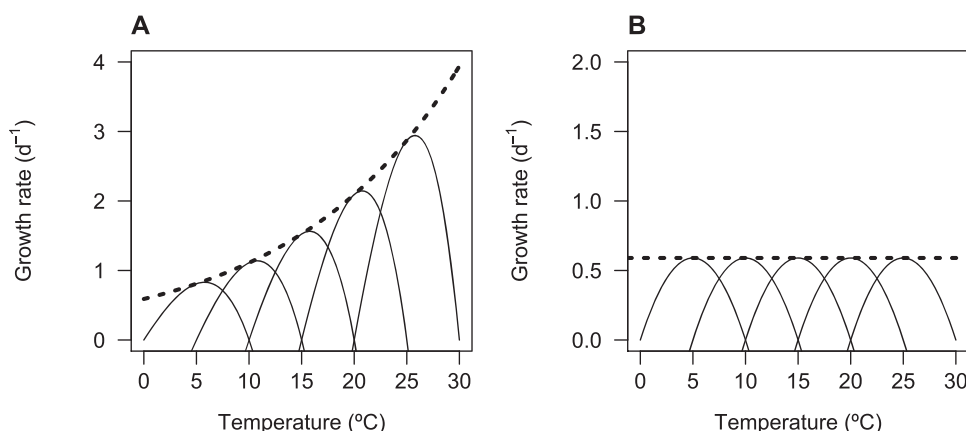


Fig. 1. Scaling from individual to whole-community temperature responses. **(A)** Under saturating irradiance, individual species/genotypes exhibit unimodal responses to temperature (solid lines), but competitive species sorting leads to an exponential response of the aggregate growth rate across a temperature gradient (dashed line). **(B)** Under light limitation, maximal growth may not increase at higher temperatures; aggregate community rates may then be insensitive to temperature even if individual species are sensitive. Note that the axes for **(A)** and **(B)** are on different scales.

The diversity of experimental results and modeling approaches highlights the need for a synthesis of data on the light–temperature interaction, which can address several important questions: Are there general rules for how light and temperature interact to determine growth, and how consistent are these patterns across a diversity of species? How might community structure be affected by the temperature responses of traits that determine competition? Can the temperature scaling of aggregate ecosystem processes be projected from trait variation across species adapted to different conditions? To address these questions, here we quantify how the parameters of the growth–irradiance curve change with temperature, and how the optimal temperature for growth changes with irradiance, for 57 marine and freshwater phytoplankton species. We quantify whether different light utilization traits have different temperature sensitivities, and whether different traits of the same species are co-adapted to the same temperature. Finally, we use a compilation of field-based primary production incubations to ask whether the effects of light and temperature on aggregate growth of natural phytoplankton communities is similar to what is predicted from lab-based trait measurements of species adapted to different temperature and irradiance regimes.

Methods

Data compilation

Previously we compiled from the literature comprehensive datasets of phytoplankton temperature traits (Thomas et al. 2012, 2016) and light utilization traits (Schwaderer et al. 2011; Edwards et al. 2015). While compiling these studies we gathered a subset of experiments that measured growth rate of a single phytoplankton isolate across a factorial manipulation of temperature and irradiance. In the current analysis, we include only those experiments where at least four irradi-

ance levels and four temperature levels were used. The median range of temperatures used in an experiment was 17°C, the narrowest range was 7°C and the broadest was 30°C. In all experiments, nutrients were not strongly limiting, and the cultures were acclimated to irradiance and temperature treatments before growth rate was measured. These criteria yielded 59 experiments from 29 publications on 57 unique species (31 freshwater and 26 marine; Supporting Information Tables A1, A2, A3). Taxonomically the species include 19 diatoms, 18 chlorophytes, 6 cyanobacteria, 3 haptophytes, 3 cryptophytes, 2 dinoflagellates, 2 desmids, and 2 chrysophytes. For all analyses, we pool marine and freshwater species to simplify presentation of the results. In our dataset marine species tend to have lower temperature optima on average, but preliminary analyses showed that the interaction between temperature and irradiance, which is the focus of this study, did not vary between these groups. Supplementary plots show the major results coded by freshwater or marine origin (Supporting Information Figs. A1–A3). Scripts for all statistical models used in the analysis are included as Supporting Information.

Growth–irradiance and growth–temperature curves

To characterize how light utilization changes with temperature, for each experiment we fit a growth–irradiance curve to the measurements from each temperature level. We used the following curve:

$$\mu(I) = \frac{\mu_{\max} I}{\frac{\mu_{\max}}{\alpha I_{\text{opt}}} I^2 + \left(1 - 2 \frac{\mu_{\max}}{\alpha I_{\text{opt}}}\right) I + \frac{\mu_{\max}}{\alpha}} \quad (1)$$

where μ is the specific growth rate (d⁻¹) as a function of the photon flux density (I , $\mu\text{mol photons m}^{-2} \text{s}^{-1}$), μ_{\max} is the maximum growth rate achieved at I_{opt} , the optimal irradiance, and α is the initial slope of the curve. In other words,

as $I \rightarrow 0$, $\mu(I) \rightarrow \alpha I$. This curve was derived by Eilers and Peeters (1988) from a dynamic model of photoinhibition of photosynthesis, and it allows us to compare across species the relative performance under limiting irradiance (α), relative performance under saturating irradiance (μ_{\max}), and the irradiance above which photoinhibition reduces growth (I_{opt}). As reviewed previously (Edwards et al. 2015), theory and experiments show that these parameters determine competitive ability and coexistence under a variety of irradiance regimes. For example, for species with equal loss rates, α should determine competitive ability under chronically low irradiance (such as that experienced at a deep chlorophyll maximum). In mixed layers, α , μ_{\max} , and I_{opt} may all be important for competitive outcomes, depending on incident irradiance and the depth of mixing (Huisman and Weissing 1994; Huisman et al. 1999; Gerla et al. 2011).

Equation 1 does not include a parameter for maintenance respiration, i.e., the growth rate when irradiance is zero. However, maintenance respiration is typically low for phytoplankton ($\sim 0.02 \text{ d}^{-1}$, Geider and Osborne 1989), and negative growth rates were only observed in four growth-irradiance relationships (out of 327 total). In addition, 95 experiments used four irradiance levels, and we did not wish to estimate a four-parameter curve from four observations. Therefore, we used the three-parameter curve and removed the four relationships with negative growth rates from the analysis. The fitted curves are given in Supporting Information S1. As described previously (Edwards et al. 2015), we used Eq. 1 instead of the curve of Platt et al. (1980) because the two curves have a very similar shape, but Eq. 1 is parameterized in terms of the traits we wish to compare across species, and often fits the data slightly better.

To compare optimum temperature for growth as a function of irradiance, we fit the following curve:

$$\mu(T) = \left[1 - \left(\frac{T-z}{\omega/2} \right) \right] a e^{bT} \quad (2)$$

where z is the midpoint of the growth curve, ω is the width of the unimodal response to temperature, and a and b jointly determine the overall height, steepness, and skewness of the curve (Norberg 2004; Thomas et al. 2012). We estimated the optimum temperature (T_{opt}) from the fitted curve by numerical optimization. For subsequent analysis, we use only those growth-temperature relationships where the estimated optimum is at least 5°C from the highest experimental temperature.

Response of light utilization traits to temperature

Exploration of the growth-irradiance curves showed that all three traits (α , μ_{\max} , I_{opt}) exhibit substantial variation with temperature for nearly all species (Supporting Information S2). For each trait about half of the relationships are unimodal, and most of the remainder are monotonically increasing, while a few are monotonically decreasing or

essentially flat. To characterize the typical shape of the temperature responses and compare the sensitivity to temperature across the three traits, we took two approaches. The first approach was to quantify how steeply the trait values rise and fall with temperature, by breaking each curve into rising and falling portions. The second approach was to characterize the mean shape of the curve using a nonparametric smoother.

To characterize the rising portion of the curve, for each experiment we selected the trait values measured at or below the temperature of the maximum trait value; we only included experiments for which there were at least two values at temperatures below the maximum, yielding a total of at least three values. To quantify the typical shape of the rising curve, we fit a generalized additive mixed model (GAMM) where the trait value was a non-parametric smooth function of temperature, and a random effect for species was included to account for the fact that species differ in their mean trait (across temperatures). Because species have different temperature optima, we standardized the temperatures so that all species had their trait maximum at the same position on the temperature axis (set to 0). We also fit a linear mixed model with $\log(\text{trait})$ as the response, which is equivalent to assuming that the trait increases exponentially with temperature. Using the fitted slope we calculated a Q_{10} coefficient for the trait. We then repeated this whole procedure for the falling portion of the curve, again only using experiments where there were at least two trait values at temperatures above the temperature of the maximum trait value.

The second approach was to characterize the typical shape of the whole temperature response curve for each trait. For this analysis, we used only those species for which the maximum trait value was not at the highest or lowest temperature (i.e., the relationship appears unimodal). Again we used a GAMM with a random effect for species, and we standardized the temperature axis so that all species had their maximum trait value at the same position (set to 0). For all of the above analyses, we only used I_{opt} estimates when the estimated I_{opt} was less than the maximum irradiance used in the experiment; otherwise there was not sufficient data to estimate I_{opt} . When comparing I_{opt} across temperatures, we only used experiments where I_{opt} could be estimated for at least four temperatures.

Response of temperature optima to irradiance

To characterize how the optimal growth temperature changes with irradiance, we fit a GAMM with T_{opt} as the response variable, a smoother for the effect of irradiance, and a random effect for species to account for differences between species in mean T_{opt} across irradiances.

Comparison of temperature optima across traits

To test whether different traits have similar temperature optima, we compared the temperature of the maximal trait values across species. We will refer to these respectively as

T_{opt}^z , T_{opt}^μ , and T_{opt}^I . It should be noted that a higher α or μ_{max} are always beneficial, all else equal, while a higher I_{opt} will reduce photoinhibition but also reduce growth at lower irradiances. Nonetheless, as shown below T_{opt}^I is correlated with T_{opt}^z and T_{opt}^μ , suggesting that species exhibit higher I_{opt} at temperatures to which they are best adapted. We performed standardized major axis regression (SMA; Warton et al. 2006) for T_{opt}^z vs. T_{opt}^μ , T_{opt}^μ vs. T_{opt}^I , and T_{opt}^z vs. T_{opt}^I . For these analyses, we only compared temperature optima when at least one of the optima was not at the highest or lowest temperature measured. Our rationale is that if two traits both peak at the highest temperature in the experiment (or the lowest temperature), there is not sufficient information to ask whether these traits have similar optima. However, if at least one trait shows a unimodal relationship to temperature, then we can ask whether the two traits peak at the same temperature or not.

Trait envelopes

To understand how the interaction between irradiance and temperature will affect whole-community growth, we quantified trait envelopes (Fig. 1) for α , μ_{max} , and I_{opt} as a function of temperature, by performing quantile regression on the trait data from all species. For each trait we fit a model where the 90th percentile of log(trait) is a linear function of temperature; this is equivalent to assuming that the 90th percentile increases exponentially with temperature. We used the 90th percentile because we are interested in the upper envelope of trait variation, but higher percentiles tend to have low statistical confidence. For comparison we also fit an ordinary least squares regression. In preliminary analyses, we also fit non-parametric curves to the 90th percentile of the data (using GAMLSS, generalized additive models for location, scale, and shape; Rigby and Stasinopoulos 2005) and to the mean of the data (using a generalized additive model, GAM). However, we found that the relationships only deviated from linear at extreme temperatures for which there was less data, and so we present the linear fits here for simplicity.

Light–temperature interactions in field incubations

To compare the patterns found in the trait envelope analyses to whole-community growth in natural systems, we used the extensive compilation of ~24,000 marine primary production observations compiled by Behrenfeld and colleagues (<http://www.science.oregonstate.edu/ocean.productivity/field.data.c14.readme.php>). This compilation contains ¹⁴C uptake measurements, from field incubations of 2–24 h duration (only a small percentage are <6 h), taken over depth profiles (range 0–175 m) at >1600 stations across a wide range of productivity and latitude (Behrenfeld and Falkowski 1997). In addition to daily carbon fixation, the dataset includes chlorophyll concentration, surface PAR, incubation PAR, latitude, longitude, date, and sea surface temperature. This information can be used to calculate chlorophyll-specific daily primary production. If the chlorophyll-to-carbon ratio (Chl:C) of the phytoplankton were known (it is not), then

phytoplankton growth rate could be approximated as the carbon-specific rate of daily carbon fixation (Eppley 1972; Marañón 2005). For our purposes, we are more interested in how the interaction between irradiance and temperature causes relative changes in growth than the absolute magnitude of growth. Therefore, we took two approaches to the issue of Chl:C, and the fact that Chl:C may change with irradiance and temperature (Cloern et al. 1995). (1) Convert Chl-specific production to specific growth rate, using a Chl:C ratio of 0.01, which is an intermediate value based on estimates for ocean phytoplankton (Behrenfeld et al. 2005); (2) assume that Chl:C varies according to the model of Behrenfeld et al. (2005), which is an empirical model of how Chl:C changes with irradiance and temperature, based on remote sensing of bulk chlorophyll and phytoplankton biomass. The model is $\text{Chl:C} = \text{Chl:C}_{\min} + (\text{Chl:C}_{\max} - \text{Chl:C}_{\min})e^{-3I}$, with $\text{Chl:C}_{\min} = 0.017 - 0.00045T$, and $\text{Chl:C}_{\max} = 0.015 + 0.00005e^{0.215T}$, and where T is temperature (°C) and I is daily irradiance ($\text{mol quanta m}^{-2} \text{ h}^{-1}$). Thus, Chl:C declines exponentially with irradiance, and the range of potential Chl:C increases with temperature. Although our approach yields only a rough estimate of phytoplankton growth rate, the large number of observations over a wide range of irradiance and temperature conditions allows us to ask whether the trait envelope predictions from our monoculture compilation are consistent with light–temperature interactions in natural communities.

Because we are interested in effects of irradiance and temperature, we excluded observations where nutrients were likely to be strongly limiting. We excluded values where nitrate concentration is expected to be <0.5 $\mu\text{mol L}^{-1}$ based on the World Ocean Atlas (Garcia et al. 2014), and we excluded values from >60° N or >40° S, which are likely to be iron-limited (Moore et al. 2013). Finally, because only sea surface temperature is reported in the dataset, we only used values from the mixed layer, based on a climatology of mixed layer depth (de Boyer Montégut et al. 2007), and we used SST to approximate temperature for all samples within the mixed layer at each station. These criteria resulted in 2090 observations for analysis.

To quantify how temperature and irradiance interact to affect our proxy of phytoplankton growth, we fit linear regressions of log(growth) vs. temperature for low-light samples (<20 $\mu\text{mol photons m}^{-2} \text{ s}^{-1}$) and for sufficient-light samples (between 100 $\mu\text{mol photons m}^{-2} \text{ s}^{-1}$ and 200 $\mu\text{mol photons m}^{-2} \text{ s}^{-1}$). We also fit a generalized additive model with a two-dimensional smoother for the interactive effect of irradiance and temperature.

Results

For all three growth-irradiance traits (α , μ_{max} , I_{opt}), nearly all species exhibit substantial variation with temperature (Supporting Information Fig. A1). About half of the

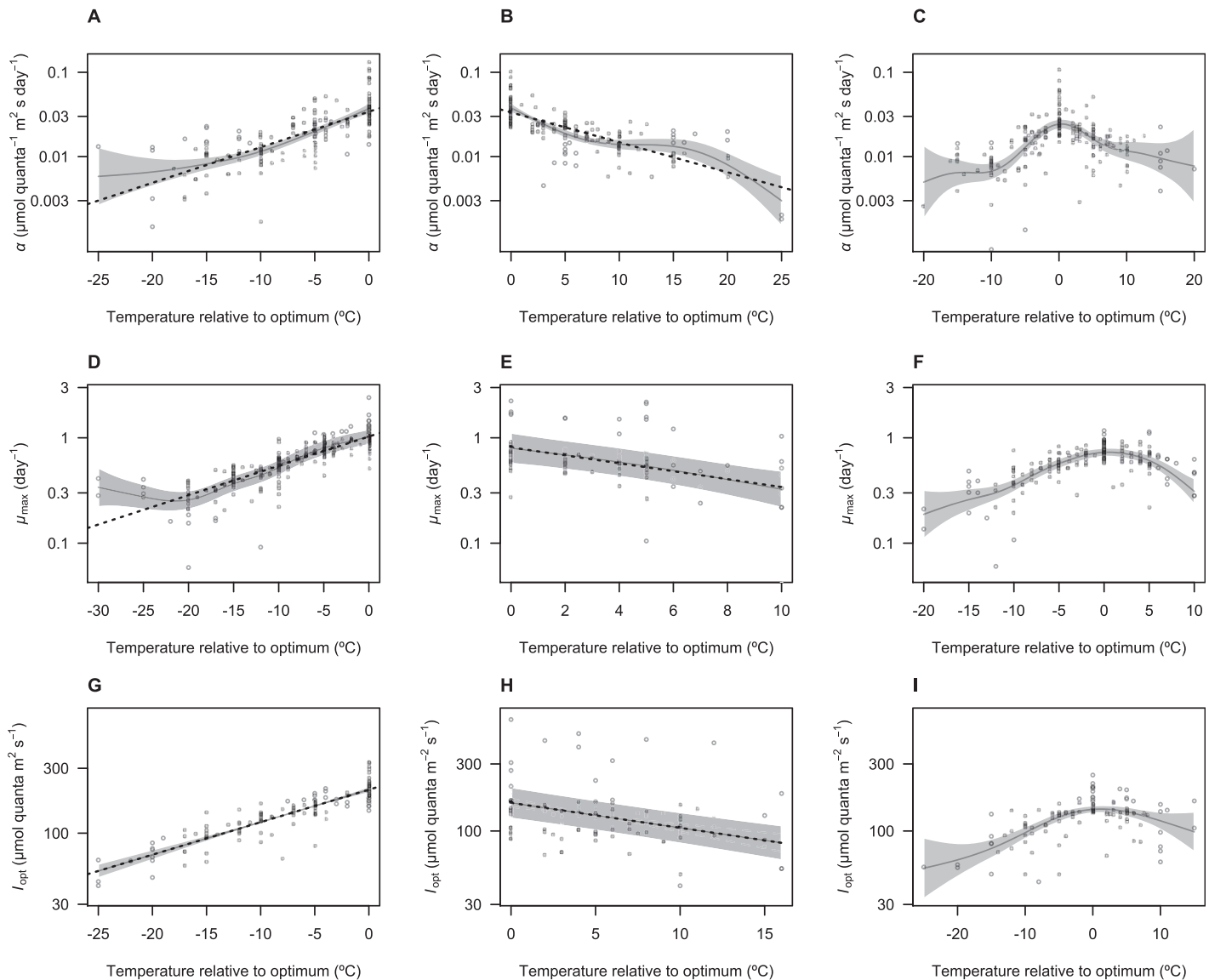


Fig. 2. Rising portion (**A, D, G**), falling portion (**B, E, H**), and full curve (**C, F, I**) for the three growth-irradiance traits as a function of temperature. The rising and falling portions are fit both as linear regressions with $\log(\text{trait})$ as the response (dashed lines) and generalized additive models (solid lines with 95% confidence bands). The plotted points are corrected, using the fitted GAMM, to remove differences between species in the mean trait value across temperatures. The x-axis uses temperature values that have been standardized, such that each species reaches its maximum trait value at 0° , as described in Methods.

relationships were unimodal, and most of the remainder are monotonically increasing, while a few are monotonically decreasing or essentially flat. Both the rising and falling portions of the curve could be approximated by an exponential relationship, for all three traits (i.e., a linear relationship between $\log(\text{trait})$ and temperature; Fig. 2). Although an exponential relationship is certainly a simplification, because the full unimodal relationships are flatter near the optimum (Fig. 2C,F,I), the near-exponential rising and falling portions are useful to characterize the sensitivity of these traits to temperature. Combining the data across species, the estimated Q_{10} values for the rising curves are 2.64, 1.90, and 1.73 for α ,

μ_{\max} , and I_{opt} , respectively (95% confidence intervals for Q_{10} are [2.17, 3.19], [1.77, 2.03], and [1.62, 1.85], respectively). The estimated Q_{10} values for proportional decrease along the falling curves are 2.26, 2.38, and 1.51 for α , μ_{\max} , and I_{opt} , respectively (95% confidence intervals for Q_{10} are [1.90, 2.69], [1.67, 3.42], and [1.32, 1.72], respectively).

Comparison of the temperatures at which growth-irradiance traits reach their maximum values shows that the three traits tend to be co-adapted to similar temperatures (Figs. 3A–C, 2C,F,I). For the temperature of peak α vs. the temperature of peak μ_{\max} , SMA regression has an intercept of -5.52 (95% CI: $[-11.2, 0.17]$), a slope of 1.06 (95% CI:

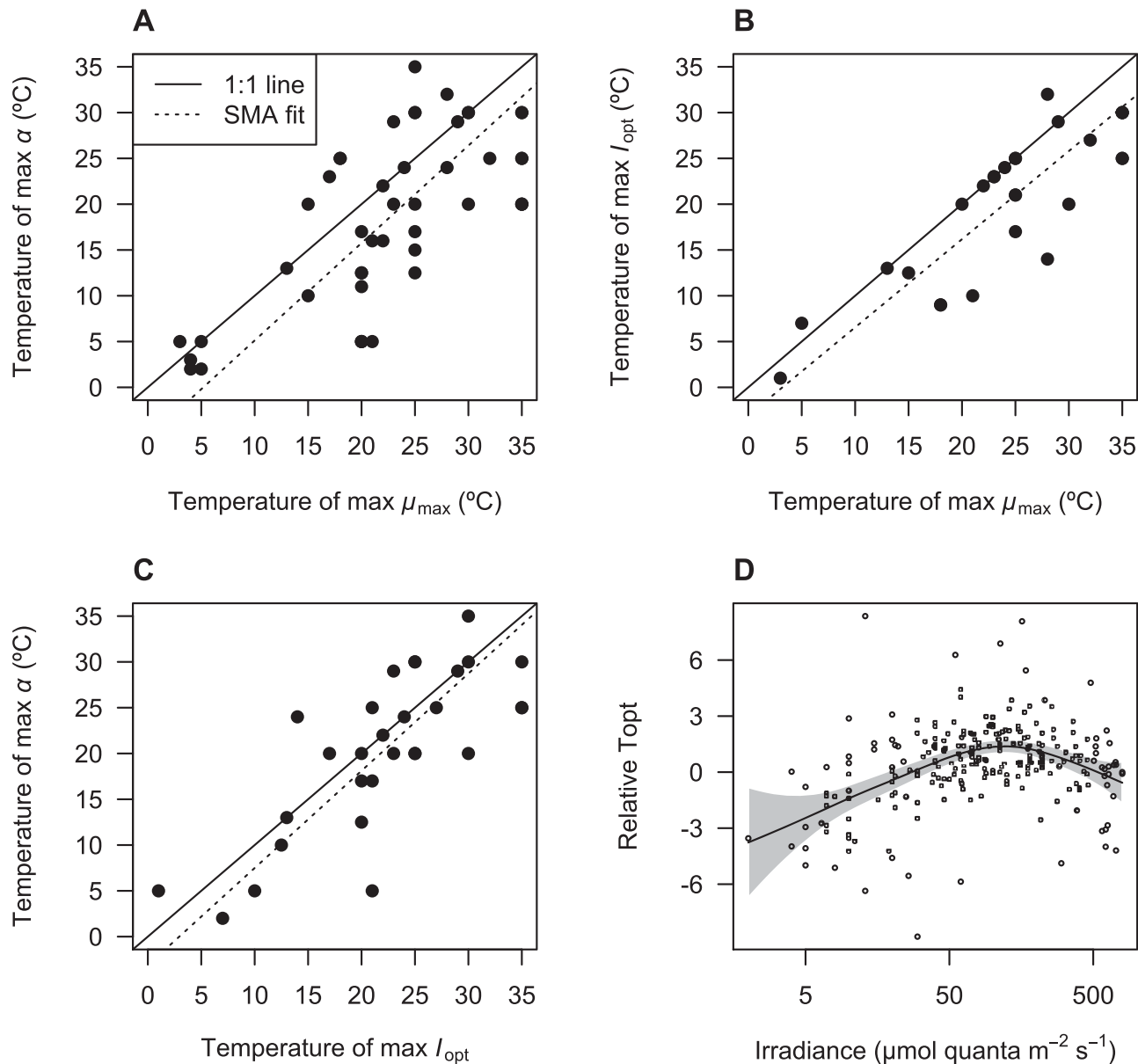


Fig. 3. (A–C) Comparison across species of temperature optima for α and μ_{\max} , I_{opt} and μ_{\max} , and α and I_{opt} , respectively. (D) Optimal temperature for growth as a function of irradiance. The y-axis in this plot is relative T_{opt} , which subtracts the mean value of T_{opt} for each species, to better visualize how T_{opt} changes with irradiance for all species. The fitted smoother is from a generalized additive model.

[0.86, 1.32]), and $R^2 = 0.48$. For the temperature of peak I_{opt} vs. the temperature of peak μ_{\max} , SMA regression has an intercept of -3.08 (95% CI: $[-8.6, 2.43]$), a slope of 0.96 (95% CI: $[0.77, 1.2]$), and $R^2 = 0.71$. For the temperature of peak α vs. the temperature of peak I_{opt} , SMA regression has an intercept of -3.12 (95% CI: $[-9.5, 3.2]$), a slope of 1.06 (95% CI: $[0.83, 1.36]$), and $R^2 = 0.59$. Therefore, the slopes of these relationships are not significantly different from 1, while the intercept for α vs. μ_{\max} is likely lower than 0, indicating that α tends to peak at a lower temperature than μ_{\max} . It may also be the case that I_{opt} tends to peak at a lower tem-

perature than μ_{\max} , because 11 values in Fig. 3B are below the 1:1 line, while only 2 are above the 1:1 line.

An analysis of how the optimal growth temperature (T_{opt}) changes with irradiance (Fig. 3D) is consistent with the differences in Fig. 3A,B. The value of T_{opt} increases by about 4 °C from the lowest irradiance to about 100 $\mu\text{mol photons m}^{-2} \text{s}^{-1}$, and then decreases by 1–2 °C at the highest irradiance.

A comparison of α values for all species across temperatures shows that the upper limit on α does not change with temperature (Fig. 4A). The regression slope for the 90th percentile of $\log_{10} \alpha$ vs. temperature is -0.0024 (95% CI: $[-0.0066, 0.015]$).

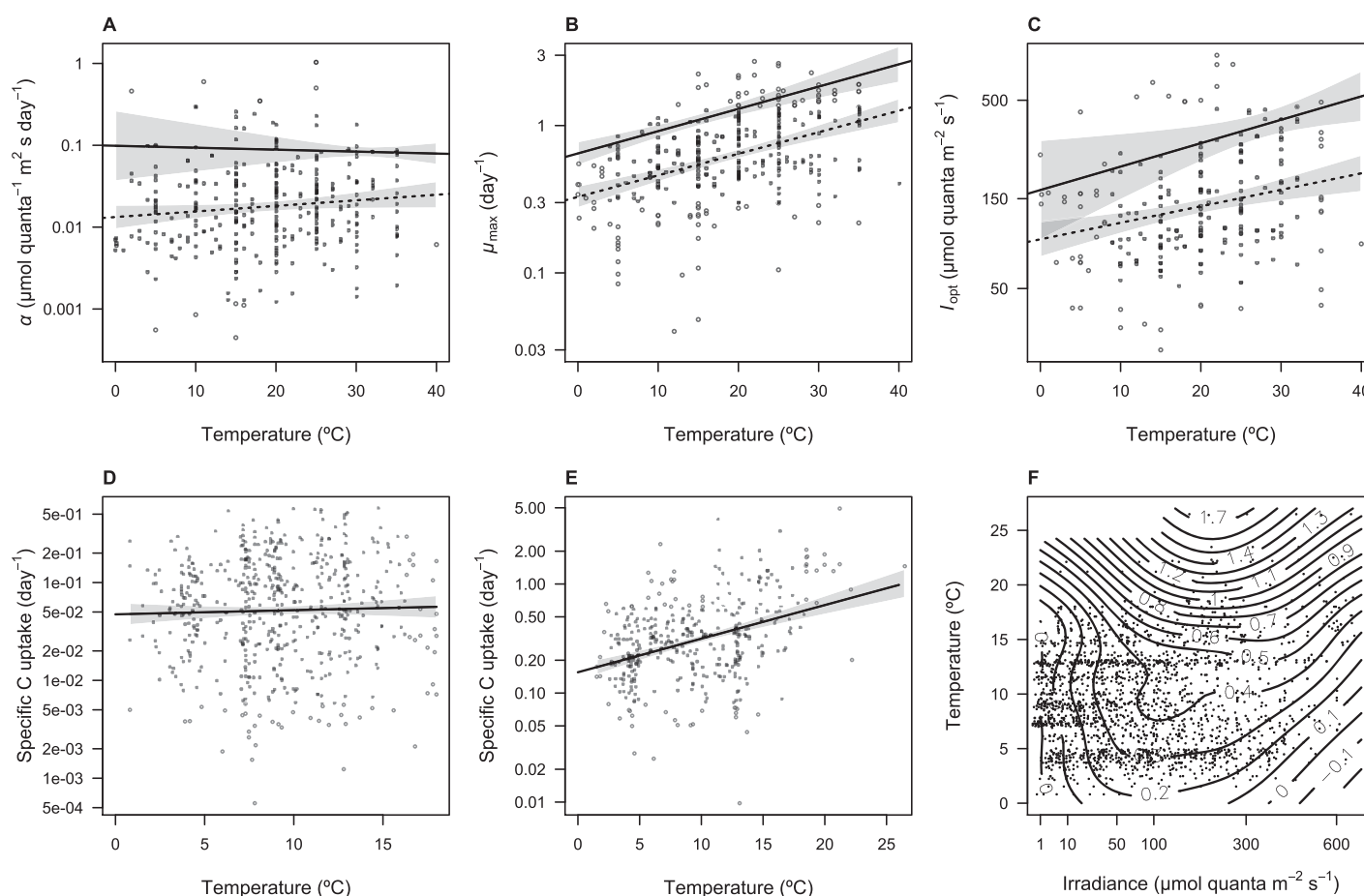


Fig. 4. (A–C) Trait envelopes for the three growth-irradiance traits across temperatures. The solid line is the quantile regression fit to the 90th percentile of all trait data for all species, the dashed line is an ordinary least squares fit to the mean of the data. (D) Whole community growth rate vs. temperature, at irradiances below 20 $\mu\text{mol photons m}^{-2} \text{s}^{-1}$. Specific growth rate is approximated using Chl-specific primary production (^{14}C uptake), with a fixed Chl: C of 0.01. (E) Whole community growth vs. temperature, at irradiances between 100 $\mu\text{mol photons m}^{-2} \text{s}^{-1}$ and 200 $\mu\text{mol photons m}^{-2} \text{s}^{-1}$. (F) Two-dimensional smoother from a GAM fit to whole community growth as a function of temperature and irradiance.

Likewise, an OLS regression through the middle of the data has a weakly increasing slope not different from zero (0.0068, 95% CI: [−0.00033, 0.014]). In contrast, the upper limit and mean of μ_{\max} increase with temperature (Fig. 4B). The 90th percentile slope for $\log_{10} \mu_{\max}$ vs. temperature is 0.015 (95% CI: [0.011, 0.019]), which corresponds to a Q_{10} of 1.42 (95% CI: [1.28, 1.56]), and the OLS slope is also 0.015 (95% CI: [0.011, 0.018]). Finally, the upper limit on I_{opt} also tends to increase with temperature (Fig. 4C). The 90th percentile slope for $\log_{10} I_{\text{opt}}$ vs. temperature is 0.012 (95% CI: [0.0052, 0.014]), which corresponds to a Q_{10} of 1.33 (95% CI: [1.13, 1.39]), and the OLS slope is 0.0088 (95% CI: [0.0042, 0.013]).

An analysis of field estimates of primary production shows that the temperature sensitivity of growth depends on irradiance. When irradiance is $\leq 20 \mu\text{mol photons m}^{-2} \text{s}^{-1}$, Chl-specific C uptake shows no trend with temperature (Fig. 4D; regression slope of $\log_{10}(\text{growth})$ vs. temperature = 0.004, 95% CI: [−0.008, 0.016]). In contrast, when irradiance is between 100 $\mu\text{mol photons m}^{-2} \text{s}^{-1}$ and 200 $\mu\text{mol photons m}^{-2} \text{s}^{-1}$,

Chl-specific C uptake increases with temperature (Fig. 4E; regression slope of $\log_{10}(\text{growth})$ vs. temperature = 0.031, 95% CI: [0.023, 0.038]; equivalent Q_{10} = 2.04, 95% CI: [1.71, 2.42]). Finally, in the field data the optimal irradiance for growth tends to increase with temperature, changing from about 100 $\mu\text{mol photons m}^{-2} \text{s}^{-1}$ to 200 $\mu\text{mol photons m}^{-2} \text{s}^{-1}$ when moving from the lowest to highest temperatures. This is most readily seen by fitting a 2D smoother for the effect of irradiance and temperature (Fig. 4F).

The patterns in Fig. 4D–F use a constant Chl:C of 0.01 to convert from Chl-specific to C-specific values. If a variable Chl:C is used instead, derived from the remote sensing model of Behrenfeld et al. (2005), the results are very similar (Supporting Information Fig. A4).

Discussion

Our compilation shows a substantial effect of temperature on the growth-irradiance relationship. Each of the

growth-irradiance parameters exhibits a unimodal temperature response that has a fairly consistent shape across species, with different species possessing different temperature optima (Figs. 1, 2). The temperature sensitivities of the traits are comparable, with each trait exhibiting a mean Q_{10} between 1.5 and 2.6 on both the rising and falling portions of the response. For the rising portion of the curve, α has a Q_{10} that is greater than the often-used values of 1.88 or 2 (95% CI: [2.17, 3.19]), while μ_{\max} has a Q_{10} that overlaps these values (95% CI: [1.77, 2.03]), and I_{opt} has a lower Q_{10} (95% CI: [1.62, 1.85]). This means that for individual species, the light-limited growth rate is at least as sensitive to temperature as the light-saturated growth rate, and susceptibility to photoinhibition also changes significantly with temperature. For any particular species the three traits tend to have similar temperature optima, but on average the optimum for α is $\sim 5^\circ\text{C}$ lower than the optimum for μ_{\max} , and the optimum for I_{opt} lies between these. Likewise, the optimal temperature for growth increases by about 4°C from the lowest irradiance to about $100 \mu\text{mol photons m}^{-2} \text{ s}^{-1}$, and then decreases by $1\text{--}2^\circ$ at the highest irradiance.

Temperature will change community structure in part by altering the values of traits that determine resource (e.g., light) competition. The responses of α , I_{opt} and μ_{\max} to temperature imply that competitive ability under either chronic light limitation such as at a DCM (where α approximates competitive ability) or fluctuating light limitation such as in a mixed layer (where α , μ_{\max} , and I_{opt} may contribute to competitive ability) will be temperature-sensitive, leading to distinct temperature niches under competition for light. It may also be the case that a transition from saturating to limiting irradiance causes species' temperature niches to shift toward cooler temperatures, i.e., it decreases their ability to tolerate higher temperatures. This shift could be adaptive, because temperature and irradiance are positively correlated over depth, and over time in seasonal environments. In addition, Thomas et al. (2012) found that T_{opt} for marine isolates tends to be $\sim 4^\circ\text{C}$ higher than mean SST at the isolation location, which may be due to widespread (co)limitation of growth by irradiance, which reduces T_{opt} below that measured under sufficient irradiance. Nutrient limitation may have a similar effect on species' thermal optima (Thomas et al. unpubl.). These predictions can be tested in field and lab experiments by quantifying how community composition changes in response to factorial combinations of light and temperature.

Ecosystem processes such as primary production and element cycling depend on aggregate community responses to environmental forcing. Predicting aggregate responses to temperature (or other factors) is more challenging than predicting species- or genotype-level responses, because aggregate patterns emerge from the outcome of complex interactions among diverse actors. If a single trait determines competitive outcomes along an environmental gradient, then in theory the upper envelope of that trait will quantify how aggregate

function changes along the gradient (Norberg 2004). The compiled monoculture data shows that neither the upper envelope nor the mean of α changes across temperatures (Fig. 4A). In contrast, the upper envelope and mean of μ_{\max} both increase exponentially with temperature, consistent with previous findings (Eppley 1972; Bissinger et al. 2008), and I_{opt} also increases with temperature (Fig. 4B,C). From these patterns, we can predict that whole-community growth should be temperature-insensitive under strong light limitation but temperature-sensitive under saturating light, and intermediate light limitation will yield a dampened temperature sensitivity. In addition, the optimal irradiance should increase with temperature. It is interesting that α for individual species is quite temperature-sensitive, while the upper envelope for α is not, which suggests substantial species turnover with little ecosystem-level effect across a temperature gradient, at the lowest irradiances (Fig. 1B). The analysis of primary production data is consistent with the predictions from trait envelopes. Whole-community growth (approximated as Chl-specific C uptake) is temperature-insensitive under low irradiance, but increases exponentially with temperature under moderate or high irradiance, and the optimal irradiance increases modestly with temperature (Fig. 4D-F). Although ^{14}C incubation data is a rough proxy of the actual bulk growth rate, it is encouraging that predictions from the lab-measured trait data are consistent with field patterns.

One difference between the lab and field patterns is the slope of the growth response under saturating irradiance, which has a Q_{10} of 1.42 for the trait envelope but a Q_{10} of 2.04 in the field data. This may be due to insufficient sampling of species adapted to high temperatures in the trait compilation or biases in the field data that change with temperature; using the 99th percentile of the data instead of the 90th percentile yields a similar Q_{10} of 1.44. Prior compilations of maximal growth rates using a larger number of species have found a Q_{10} of 1.88 (Eppley 1972; Bissinger et al. 2008), which is closer to the slope observed in the field data and supports the upper envelope for μ_{\max} as a predictor of light-saturated growth rate. Studies applying the "metabolic theory of ecology" have argued that primary production has a temperature sensitivity largely determined by the activation energy of Rubisco (0.32 eV), which is thought to limit the light-saturated rate of photosynthesis (Allen et al. 2005; López-Urrutia et al. 2006). This activation energy corresponds approximately to a Q_{10} of 1.64, which is intermediate between the lab and field sensitivities under saturating light in our study. Our results indicate that the metabolic theory approach is likely not suitable for phytoplankton when light limits growth. Nonetheless, it is possible that under sufficient light the temperature response of phytoplankton growth is driven by Rubisco. However, it is not clear how to reconcile this enzyme-specific view with unimodal species-level responses, which scale up to produce monotonic

aggregate responses. Furthermore, this framework does not account for responses to excess irradiance.

Prior studies have found conflicting results for the effect of temperature on aggregate phytoplankton growth or specific primary production. Chen et al. (2012) found that growth rate in marine dilution experiments increases exponentially with temperature, and Regaudie-de-Gioux and Duarte (2012) found the same using a compilation of Chl-specific gross primary production in the open ocean. In contrast, Marañón et al. (2014) found that resource supply across ocean regions explains phytoplankton growth with little direct role for temperature, and De Castro and Gaedke (2008) found that seasonal variation in Chl-specific photosynthesis in Lake Constance was unrelated to temperature. Our results suggest that conflicting patterns can be reconciled by accounting for resource supply, with light limitation diminishing the temperature-sensitivity of bulk growth. Nutrient limitation may have a similar dampening effect, as seen in mesocosm experiments (Staehr and Sand-Jensen 2006; O'Connor et al. 2009), although we currently lack sufficient culture studies to make predictions based on trait envelopes for nutrient competition. Due to the ubiquity of resource limitation (or co-limitation) in marine and fresh waters, it will be essential to better quantify how temperature and resources interact, and how temperature also modulates grazers and pathogens (e.g., Chen et al. 2012). It will also be important to better quantify temperature effects on photosynthesis vs. respiration, particularly under low irradiance. The data compiled here did not permit an analysis of respiratory costs, but if respiration has a greater temperature sensitivity than light-limited photosynthesis, this could have important effects on patterns of net primary production (e.g., López-Urrutia et al. 2006).

Based on our data synthesis, we make some recommendations below for modeling phytoplankton growth at the species and community levels. Models of phytoplankton growth often use a simple exponential term to account for the effect of temperature (Blackford et al. 2004; Taucher and Oschlies 2011). If the phytoplankton variable is intended to represent bulk phytoplankton, or aggregate growth of a diverse functional group, then such a monotonic temperature effect is appropriate, but only under sufficient irradiance. Therefore, it would be appropriate to use a functional form where the maximum growth rate has an exponential or Arrhenius-type temperature dependence, but the initial slope of the irradiance response is temperature-insensitive. An interaction between irradiance and temperature is a feature of the photoacclimation models of Geider et al. (1997, 1998), which have been used in a variety of biogeochemical models (e.g., Moore et al. 2002; Stock et al. 2014). In these models, the maximum Chl-specific rate of photosynthesis (P_m^C) increases with temperature but the initial slope of Chl-specific photosynthesis vs. irradiance (α^{chl}) is insensitive to temperature. The Chl:C ratio (θ) also depends on temperature via a dependence on P_m^C . Under these assumptions, specific growth rate is essen-

tially temperature-insensitive at $1 \mu\text{mol photons m}^{-2} \text{ s}^{-1}$, weakly temperature-sensitive at $10 \mu\text{mol photons m}^{-2} \text{ s}^{-1}$, and strongly temperature sensitive at $100 \mu\text{mol photons m}^{-2} \text{ s}^{-1}$ (Supporting Information Fig. A5). Therefore, use of this model to represent aggregate growth is largely consistent with observed light-temperature interactions, although the temperature-sensitivity may arise at too low of an irradiance, and, in addition, the model does not account for photoinhibition. In contrast to monotonic temperature effects, models of individual phytoplankton populations, or models that include a diversity of phytoplankton species (e.g., Dutkiewicz et al. 2013), would be made most realistic by incorporating unimodal temperature functions for growth-irradiance parameters. A diversity of species adapted to different temperature regimes can be implemented by making the parameters follow the trait envelopes in Fig. 4. An example of a growth-irradiance model with temperature-dependent parameters is given in Supporting Information S3.

Through effects on stratification, global warming is expected to decrease nutrient supply to the euphotic zone while alleviating light limitation (Sarmiento et al. 2004). The role of the direct effects of temperature on plankton, and how these interact with resource limitation, are less clear. The results presented here suggest that the interaction of temperature and irradiance is substantial, with consequences for the niches of individual species, the structure of communities, and key ecosystem rates. Important next steps include testing these patterns in the field, integrating these interactions with effects of CO_2 , nutrients, and grazers, and incorporating the empirical patterns in ecosystem models.

References

- Allen, A. P., J. F. Gillooly, and J. H. Brown. 2005. Linking the global carbon cycle to individual metabolism. *Funct. Ecol.* **19**: 202–213. doi:[10.1111/j.1365-2435.2005.00952.x](https://doi.org/10.1111/j.1365-2435.2005.00952.x)
- Behrenfeld, M., and P. G. Falkowski. 1997. A consumer's guide to phytoplankton primary productivity models. *Limnol. Oceanogr.* **42**: 1479–1491. doi:[10.1029/2004GB002299](https://doi.org/10.1029/2004GB002299)
- Behrenfeld, M. J., E. Boss, D. A. Siegel, and D. M. Shea. 2005. Carbon-based ocean productivity and phytoplankton physiology from space. *Global Biogeochem. Cycles* **19**: GB1006. doi:[10.1029/2004GB002299](https://doi.org/10.1029/2004GB002299)
- Bissinger, J. E., D. J. S. Montagnes, and J. Sharples. 2008. Predicting marine phytoplankton maximum growth rates from temperature: Improving on the Eppley curve using quantile regression. *Limnol. Oceanogr.* **53**: 487–493. doi:[10.4319/lo.2008.53.2.0487](https://doi.org/10.4319/lo.2008.53.2.0487)
- Blackford, J. C., J. I. Allen, and F. J. Gilbert. 2004. Ecosystem dynamics at six contrasting sites: A generic modelling study. *J. Mar. Syst.* **52**: 191–215. doi:[10.1016/j.jmarsys.2004.02.004](https://doi.org/10.1016/j.jmarsys.2004.02.004)
- Boyd, P., S. Lennartz, D. Glover, and S. Doney. 2015. Biological ramifications of climate-change-mediated oceanic

- multi-stressors. *Nat. Clim. Chang.* **5**: 71–79. doi:[10.1038/NCLIMATE2441](https://doi.org/10.1038/NCLIMATE2441)
- Chen, B., M. R. Landry, B. Huang, and H. Liu. 2012. Does warming enhance the effect of microzooplankton grazing on marine phytoplankton in the ocean? *Limnol. Oceanogr.* **57**: 519–526. doi:[10.4319/lo.2012.57.2.0519](https://doi.org/10.4319/lo.2012.57.2.0519)
- Clarke, A. 2003. Costs and consequences of evolutionary temperature adaptation. *Trends Ecol. Evol.* **18**: 573–581. doi:[10.1016/j.tree.2003.08.007](https://doi.org/10.1016/j.tree.2003.08.007)
- Cloern, J., C. Grenz, and L. Videgar-Lucas. 1995. An empirical model of the phytoplankton chlorophyll: Carbon ratio—the conversion factor between productivity and growth rate. *Limnol. Oceanogr.* **40**: 1313–1321. doi:[10.4319/lo.1995.40.7.1313](https://doi.org/10.4319/lo.1995.40.7.1313)
- Cullen, J. J. 2015. Subsurface chlorophyll maximum layers: Enduring enigma or mystery solved? *Ann. Rev. Mar. Sci.* **7**: 207–239. doi:[10.1146/annurev-marine-010213-135111](https://doi.org/10.1146/annurev-marine-010213-135111)
- Dauta, A. 1982. Conditions de développement du phytoplancton: Étude comparative du comportement de huit espèces en culture. I. Détermination des paramètres de croissance en fonction de la lumière et de la température. *Ann. Limnol.* **18**: 217–262. doi:[10.1051/limn/1982005](https://doi.org/10.1051/limn/1982005)
- Davison, I. 1991. Environmental effects on algal photosynthesis: Temperature. *J. Phycol.* **27**: 2–8. doi:[10.1111/j.0022-3646.1991.00002.x](https://doi.org/10.1111/j.0022-3646.1991.00002.x)
- de Boyer Montégut, C., J. Mignot, A. Lazar, and S. Cravatte. 2007. Control of salinity on the mixed layer depth in the world ocean: 1. General description. *J. Geophys. Res.* **112**: C06011. doi:[10.1029/2006JC003953](https://doi.org/10.1029/2006JC003953)
- De Castro, F., and U. Gaedke. 2008. The metabolism of lake plankton does not support the metabolic theory of ecology. *Oikos* **117**: 1218–1226. doi:[10.1111/j.2008.0030-1299.16547.x](https://doi.org/10.1111/j.2008.0030-1299.16547.x)
- De Stasio, B., D. K. Hill, J. M. Kleinhans, N. P. Nibbelink, and J. J. Magnuson. 1996. Potential effects of global climate change on small north-temperate lakes: Physics, fish, and plankton. *Limnol. Oceanogr.* **41**: 1136–1149. doi:[10.4319/lo.1996.41.5.1136](https://doi.org/10.4319/lo.1996.41.5.1136)
- Dell, A. I., S. Pawar, and V. M. Savage. 2014. Temperature dependence of trophic interactions are driven by asymmetry of species responses and foraging strategy. *J. Anim. Ecol.* **83**: 70–84. doi:[10.1111/1365-2656.12081](https://doi.org/10.1111/1365-2656.12081)
- Doney, S. C., and others. 2012. Climate change impacts on marine ecosystems. *Ann. Rev. Mar. Sci.* **4**: 11–37. doi:[10.1146/annurev-marine-041911-111611](https://doi.org/10.1146/annurev-marine-041911-111611)
- Duffy, J. E., and J. J. Stachowicz. 2006. Why biodiversity is important to oceanography: Potential roles of genetic, species, and trophic diversity in pelagic ecosystem processes. *Mar. Ecol. Prog. Ser.* **311**: 179–189. doi:[10.3354/meps311179](https://doi.org/10.3354/meps311179)
- Dutkiewicz, S., J. R. Scott, and M. J. Follows. 2013. Winners and losers: Ecological and biogeochemical changes in a warming ocean. *Global Biogeochem. Cycles* **27**: 463–477. doi:[10.1002/gbc.20042](https://doi.org/10.1002/gbc.20042)
- Edwards, K. F., E. Litchman, and C. A. Klausmeier. 2013a. Functional traits explain phytoplankton community structure and seasonal dynamics in a marine ecosystem. *Ecol. Lett.* **16**: 56–63. doi:[10.1111/ele.12012](https://doi.org/10.1111/ele.12012)
- Edwards, K. F., E. Litchman, and C. A. Klausmeier. 2013b. Functional traits explain phytoplankton responses to environmental gradients across lakes of the United States. *Ecology* **94**: 1626–1635. doi:[10.1890/12-1459.1](https://doi.org/10.1890/12-1459.1)
- Edwards, K. F., M. K. Thomas, C. A. Klausmeier, and E. Litchman. 2015. Light and growth in marine phytoplankton: Allometric, taxonomic, and environmental variation. *Limnol. Oceanogr.* **60**: 540–552. doi:[10.1002/lno.10033](https://doi.org/10.1002/lno.10033)
- Eilers, P. H. C., and J. C. H. Peeters. 1988. A model for the relationship between light intensity and the rate of photosynthesis in phytoplankton. *Ecol. Modell.* **42**: 199–215. doi:[10.1016/0304-3800\(88\)90057-9](https://doi.org/10.1016/0304-3800(88)90057-9)
- Eppley, R. 1972. Temperature and phytoplankton growth in the sea. *Fish. Bull.* **70**: 1063–1085.
- Falkowski, P., R. Barber, and V. Smetacek. 1998. Biogeochemical controls and feedbacks on ocean primary production. *Science* **281**: 200–206. doi:[10.1126/science.281.5374.200](https://doi.org/10.1126/science.281.5374.200)
- Fennel, K., and E. Boss. 2003. Subsurface maxima of phytoplankton and chlorophyll: Steady-state solutions from a simple model. *Limnol. Oceanogr.* **48**: 1521–1534. doi:[10.4319/lo.2003.48.4.1521](https://doi.org/10.4319/lo.2003.48.4.1521)
- Field, C., M. Behrenfeld, J. Randerson, and P. Falkowski. 1998. Primary production of the biosphere: Integrating terrestrial and oceanic components. *Science* **281**: 237–240. doi:[10.1126/science.281.5374.237](https://doi.org/10.1126/science.281.5374.237)
- Geider, R. J., and B. A. Osborne. 1989. Respiration and microalgal growth: A review of the quantitative relationship between dark respiration and growth. *New Phytol.* **112**: 327–341. doi:[10.1111/j.1469-8137.1989.tb00321.x](https://doi.org/10.1111/j.1469-8137.1989.tb00321.x)
- Geider, R. J., H. L. MacIntyre, and T. M. Kana. 1997. Dynamic model of phytoplankton growth and acclimation: Responses of the balanced growth rate and the chlorophyll a:carbon ratio to light, nutrient-limitation and temperature. *Mar. Ecol. Prog. Ser.* **148**: 187–200. doi:[10.3354/meps148187](https://doi.org/10.3354/meps148187)
- Geider, R., H. L. MacIntyre, and T. Kan. 1998. A dynamic regulatory model of phytoplanktonic acclimation to light, nutrients, and temperature. *Limnol. Oceanogr.* **43**: 679–694. doi:[10.4319/lo.1998.43.4.0679](https://doi.org/10.4319/lo.1998.43.4.0679)
- Gerla, D. J., W. M. Mooij, and J. Huisman. 2011. Photoinhibition and the assembly of light-limited phytoplankton communities. *Oikos* **120**: 359–368. doi:[10.1111/j.1600-0706.2010.18573.x](https://doi.org/10.1111/j.1600-0706.2010.18573.x)
- Huisman, J., and F. J. Weissing. 1994. Light-limited growth and competition in well-mixed aquatic environments: An elementary model. *Ecology* **75**: 507–520. doi:[10.2307/1939554](https://doi.org/10.2307/1939554)
- Huisman, J., R. R. Jonker, C. Zonneveld, and F. Weissing. 1999. Competition for light between phytoplankton species: Experimental tests of mechanistic theory. *Ecology*

- 80:** 211–222. doi:10.1890/0012-9658(1999)080[0211:CFLBPS]2.0.CO;2
- Johnson, Z. I., E. M. S. Woodward, and S. W. Chisholm. 2006. Niche partitioning among *Prochlorococcus* ecotypes along ocean-scale environmental gradients. *Science* **311**: 1737–1740. doi:10.1126/science.1118052
- Kingsolver, J. G. 2009. The well-temperated biologist. (American Society of Naturalists Presidential Address). *Am. Nat.* **174**: 755–768. doi:10.1086/648310
- Kordas, R. L., C. D. G. Harley, and M. I. O'Connor. 2011. Community ecology in a warming world: The influence of temperature on interspecific interactions in marine systems. *J. Exp. Mar. Biol. Ecol.* **400**: 218–226. doi:10.1016/j.jembe.2011.02.029
- Lancelot, C., and others. 1993. Factors controlling phytoplankton ice-edge blooms in the marginal ice-zone of the northwestern Weddell Sea during sea ice retreat 1988: Field observations and mathematical modelling. *Polar Biol.* **13**: 377–387. doi:10.1007/BF01681979
- Langdon, C. 1988. On the causes of interspecific differences in the growth-irradiance relationship for phytoplankton. II. A general review. *J. Plankton Res.* **10**: 1291–1312. doi:10.1093/plankt/10.6.1291
- López-Urrutia, A., E. San Martín, R. P. Harris, and X. Irigoien. 2006. Scaling the metabolic balance of the oceans. *Proc. Natl. Acad. Sci. USA* **103**: 8739–8744. doi:10.1073/pnas.0601137103
- López-Urrutia, A., and X. A. G. Morán. 2007. Resource limitation of bacterial production distorts the temperature dependence of oceanic carbon cycling. *Ecology* **88**: 817–822. doi:10.1890/06-1641
- Marañón, E. 2005. Phytoplankton growth rates in the Atlantic subtropical gyres. *Limnol. Oceanogr.* **50**: 299–310. doi:10.4319/lo.2005.50.1.0299
- Marañón, E., P. Cermeño, M. Latasa, and R. D. Tadonlélé. 2012. Temperature, resources, and phytoplankton size structure in the ocean. *Limnol. Oceanogr.* **57**: 1266–1278. doi:10.4319/lo.2012.57.5.1266
- Marañón, E., P. Cermeño, M. Huete-Ortega, D. C. López-Sandoval, B. Mouriño-Carballido, and T. Rodríguez-Ramos. 2014. Resource supply overrides temperature as a controlling factor of marine phytoplankton growth. *PLoS One* **9**: e99312. doi:10.1371/journal.pone.0099312
- Montagnes, D. J. S., S. A. Kimmance, and D. Atkinson. 2003. Using Q10: Can growth rates increase linearly with temperature? *Aquat. Microb. Ecol.* **32**: 307–313. doi:10.3354/ame032307
- Moore, J., S. Doney, and J. Kleypas. 2002. An intermediate complexity marine ecosystem model for the global domain. *Deep-Sea Res. II* **49**: 403–462.
- Moore, C. M., and others. 2013. Processes and patterns of oceanic nutrient limitation. *Nat. Geosci.* **6**: 701–710. doi:10.1038/ngeo1765
- Morán, X. A. G., Á. López-Urrutia, A. Calvo-Díaz, and W. K. W. Li. 2010. Increasing importance of small phytoplankton in a warmer ocean. *Glob. Chang. Biol.* **16**: 1137–1144. doi:10.1111/j.1365-2486.2009.01960.x
- Nicklisch, A., T. Shatwell, and J. Kohler. 2008. Analysis and modelling of the interactive effects of temperature and light on phytoplankton growth and relevance for the spring bloom. *J. Plankton Res.* **30**: 75–91. doi:10.1093/plankt/fbm099
- Norberg, J. 2004. Biodiversity and ecosystem functioning: A complex adaptive systems approach. *Limnol. Oceanogr.* **49**: 1269–1277. doi:10.4319/lo.2004.49.4_part_2.1269
- O'Connor, M. I., M. F. Piehler, D. M. Leech, A. Anton, and J. F. Bruno. 2009. Warming and resource availability shift food web structure and metabolism. *PLoS biology* **7**: e1000178.
- O'Connor, M. I., B. Gilbert, and C. J. Brown. 2011. Theoretical predictions for how temperature affects the dynamics of interacting herbivores and plants. *Am. Nat.* **178**: 626–638. doi:10.1086/662171
- Palmisano, A. C., J. B. Soohoo, and C. W. Sullivan. 1987. Effects of four environmental variables on photosynthesis-irradiance relationships in Antarctic sea-ice microalgae. *Mar. Biol.* **306**: 299–306. doi:10.1007/BF00392944
- Platt, T., C. L. Gallegos, and W. G. Harrison. 1980. Photoinhibition of photosynthesis in natural assemblages of marine phytoplankton. *J. Mar. Res.* **38**: 103–111.
- Raven, J., and R. Geider. 1988. Temperature and algal growth. *New Phytol.* **110**: 441–461. doi:10.1111/j.1469-8137.1988.tb00282.x
- Regaudie-de-Gioux, A., and C. M. Duarte. 2012. Temperature dependence of planktonic metabolism in the ocean. *Global Biogeochem. Cycles* **26**: GB1015. doi:10.1029/2010GB003907
- Rigby, R., and D. Stasinopoulos. 2005. Generalized additive models for location, scale, and shape. *J. Roy Statist Soc. Series C* **54**: 507–554.
- Rodríguez, F., E. Derelle, L. Guillou, F. Le Gall, D. Vaultot, and H. Moreau. 2005. Ecotype diversity in the marine picoeukaryote *Ostreococcus* (Chlorophyta, Prasinophyceae). *Environ. Microbiol.* **7**: 853–859. doi:10.1111/j.1462-2920.2005.00758.x
- Sarmiento, J. L., R. Slater, R. Barber, L. Bopp, S. C. Doney, a. C. Hirst, J. Kleypas, R. Matear, U. Mikolajewicz, P. Monfray, V. Soldatov, S. a. Spall, and R. Stouffer. 2004. Response of ocean ecosystems to climate warming. *Global Biogeochem Cy* **18**.
- Schwaderer, A. S., K. Yoshiyama, P. de Tezanos Pinto, N. G. Swenson, C. A. Klausmeier, and E. Litchman. 2011. Eco-evolutionary differences in light utilization traits and distributions of freshwater phytoplankton. *Limnol. Oceanogr.* **56**: 589–598. doi:10.4319/lo.2011.56.2.0589

- Six, C., Z. V. Finkel, A. J. Irwin, and D. A. Campbell. 2007. Light variability illuminates niche-partitioning among marine Picocyanobacteria. *PLoS One* **2**: e1341. doi:[10.1371/journal.pone.0001341](https://doi.org/10.1371/journal.pone.0001341)
- Staehr, P. A., and K. Sand-Jensen. 2006. Seasonal changes in temperature and nutrient control of photosynthesis, respiration and growth of natural phytoplankton communities. *Freshw. Biol.* **51**: 249–262. doi:[10.1111/j.1365-2427.2005.01490.x](https://doi.org/10.1111/j.1365-2427.2005.01490.x)
- Stock, C. A., J. P. Dunne, and J. G. John. 2014. Global-scale carbon and energy flows through the marine planktonic food web: An analysis with a coupled physical–biological model. *Prog. Oceanogr.* **120**: 1–28. doi:[10.1016/j.pocean.2013.07.001](https://doi.org/10.1016/j.pocean.2013.07.001)
- Talmy, D., J. Blackford, N. J. Hardman-Mountford, A. J. Dumbrell, and R. J. Geider. 2013. An optimality model of photoadaptation in contrasting aquatic light regimes. *Limnol. Oceanogr.* **58**: 1802–1818. doi:[10.4319/lo.2013.58.5.1802](https://doi.org/10.4319/lo.2013.58.5.1802)
- Taucher, J., and A. Oschlies. 2011. Can we predict the direction of marine primary production change under global warming? *Geophys. Res. Lett.* **38**: L02603. doi:[10.1029/2010GL045934](https://doi.org/10.1029/2010GL045934)
- Thomas, M. K., C. T. Kremer, C. A. Klausmeier, and E. Litchman. 2012. A global pattern of thermal adaptation in marine phytoplankton. *Science* **338**: 1085–1088. doi:[10.1126/science.1224836](https://doi.org/10.1126/science.1224836)
- Thomas, M. K., C. T. Kremer, and E. Litchman. 2016. Environment and evolutionary history determine the global biogeography of phytoplankton temperature traits. *Glob. Ecol. Biogeogr.* **25**: 75–86.
- Vasseur, D. A., and K. S. McCann. 2005. A mechanistic approach for modeling temperature-dependent consumer–resource dynamics. *Am. Nat.* **166**: 184–198.
- Verity, P. 1982. Effects of temperature, irradiance, and day-length on the marine diatom *Leptocylindrus danicus* Cleve. IV. Growth. *J. Exp. Mar. Biol. Ecol.* **60**: 209–222. doi:[10.1016/0022-0981\(82\)90160-5](https://doi.org/10.1016/0022-0981(82)90160-5)
- Warton, D. I., I. J. Wright, D. S. Falster, and M. Westoby. 2006. Bivariate line-fitting methods for allometry. *Biol. Rev. Camb. Philos. Soc.* **81**: 259–291. doi:[10.1017/S1464793106007007](https://doi.org/10.1017/S1464793106007007)
- Worden, A. Z., M. J. Follows, S. J. Giovannoni, S. Wilken, A. E. Zimmerman, and P. J. Keeling. 2015. Rethinking the marine carbon cycle: Factoring in the multifarious lifestyles of microbes. *Science* **347**: 735.
- Xu, L., D. D. Baldocchi, and J. Tang. 2004. How soil moisture, rain pulses, and growth alter the response of ecosystem respiration to temperature. *Global Biogeochem. Cycles* **18**: GB4002. doi:[10.1029/2004GB002281](https://doi.org/10.1029/2004GB002281)

Acknowledgments

We thank two anonymous reviewers for helpful comments. This research was in part supported by the NSF grants OCE-0928819 and CBET-1134215 to EL and CAK and DEB 0845932 to EL. This is Kellogg Biological Station contribution #1915.

Submitted 6 November 2015

Revised 3 February 2016

Accepted 8 February 2016

Associate editor: Heidi Sosik